Homework #2

Hover Analysis (continued)

Table of Contents

List of Tables

List of Figures

List of Equations

1. Problem Definition

Given an airfoil rotor with the following characteristics:

- s = 0.1
- q_{tw} = -8 degrees
- B = 0.97
- k = 1.1
- Cutout = 7%
- C_{do} = 0.01 (for simple performance estimate)
- a = 5.7

1) Compute and plot the inflow ratio for the four cases shown on Figure 2.9 (Johnson).

2) Compute the hovering performance plot for the rotor as in Figure 2.11 (Johnson).

3) Evaluate the reduction in power for a 3:1 tapered blade at a C_T/σ = 0.07

2. Procedure

This procedure utilized to solve this problem utilizes much of the same elements of HW#1. For the Blade Element Theory (BE) calculations, the following assumptions that were utilized:

- Uniform inflow (l_i = constant).
- Constant chord.
- Root cutout = 7%.
- Constant density.
- Neglect compressibility effects (C_l vs. a is linear).
- $V + v << \Omega r$ (utilized in simplifying V_{app}).

For the simple performance estimate, all of the same assumptions were utilized (with modifications to performance equations utilizing k and C_{do}. Combined Blade Element Theory (CBE) calculations also utilize the same assumptions, except for two: uniform inflow, and for the tapered scenario, constant chord. Both λ and chord will vary in the CBE tapered blade analysis.

With these assumptions, a procedure to determine the necessary data was executed. An Excel spreadsheet, located in Annex A, contains all calculations.

2.1. Part 1)

The inflow ratio, λ, was calculated for the four cases as shown in the equations below:

$$l_i = \frac{v}{\Omega R} = \sqrt{\frac{C_T}{2}}$$

Equation 2-1: Inflow (Ideal Rotor)

$$l_i = \frac{v}{\Omega R} = k\sqrt{\frac{C_T}{2}}$$

Equation 2-2: Inflow (Empirical Solution)

$$l_i = \frac{s a}{16}\left[\sqrt{1+\frac{32}{s a} q x} - 1\right]$$

Equation 2-3: Inflow (Combined Blade Element Theory)

Upon calculating the inflow ratios at eleven equally spaced blade stations (cutout to tip, for each of the four cases), the data was graphed in Figure 2-1 below. It was necessary to assume a collective input of ten degrees in order to obtain appropriate inflows as depicted in Figure 2-9 of Johnson. As expected, the CBE twist and no twist solutions cross at x = 0.75. This spanwise distribution of inflow clearly shows the inaccuracies of the uniform inflow assumption utilized in BE Theory, especially at blade stations inboard of 0.5x.

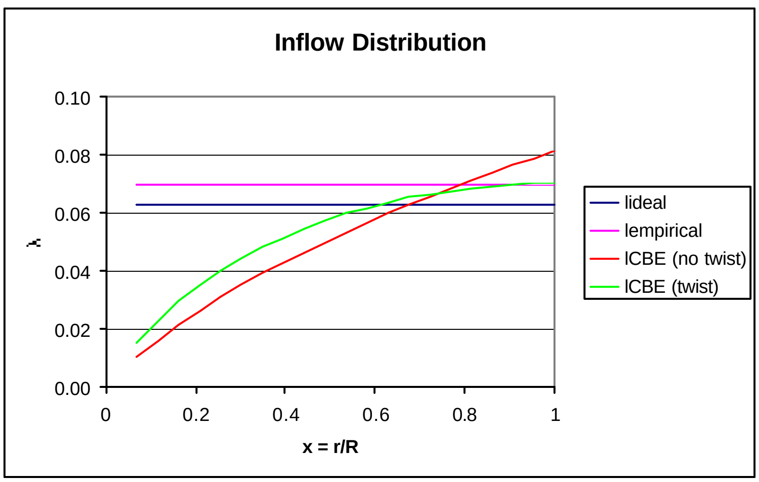

Figure 2-1: Spanwise Inflow Distribution

2.2. Part 2)

2.2.1. Simple Performance Estimate

The following equation was utilized for calculating the C_P at each of the five estimated values of C_T/s. The assumed values were 0.02, 0.04, 0.06, 0.0, and 0.1. This data was extracted from Figures 2-10 and 2-11 in Johnson.

$$C_P = k\frac{C_T^{3/2}}{\sqrt{2}} + s\,\frac{C_{d_o}}{8}$$

Equation 2-4: Simple Estimate C_P

The empirical k factor used in this estimate was 1.1. This value was assumed to account for the three types of losses not accounted for in Blade Element Theory:

- Tip Losses (≅ 2-4%)
- Non-Uniform Inflow (≅ 8-12%)
- Swirl (≅ 1-2%)

2.2.2. Blade Element Theory

First, the blade was divided into 10 elements for analysis as depicted in Figure 2-2.

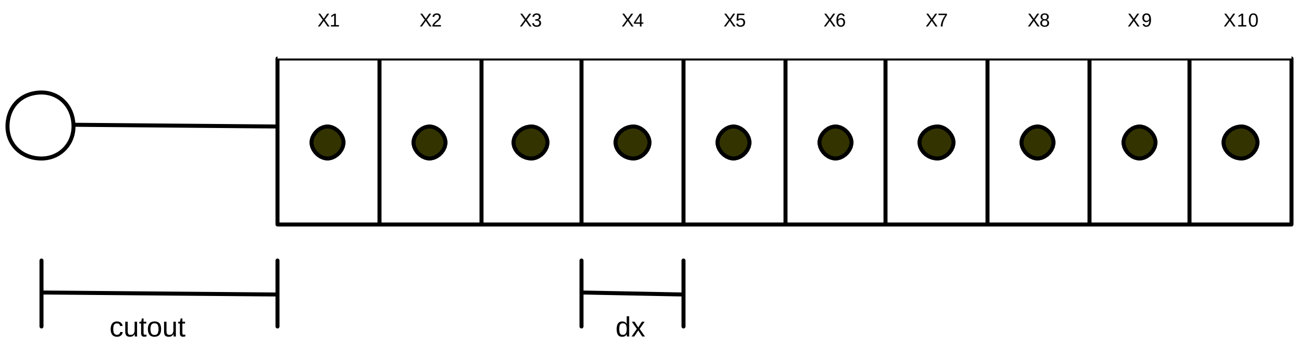

Figure 2-2: Blade Element Breakdown

From Figure 2-2, and utilizing Equation 2-5, Equation 2-6 and Equation 2-7, the blade elements are defined.

$$dx = (1 - cutout)/10$$

Equation 2-5: Blade Differential Elements

$$x_{n=1} = cutout + \frac{dx}{2}$$

Equation 2-6: Initial Blade Station

$$x_{n\,(for\,n=2..10)} = x_{n-1} + dx$$

Equation 2-7: Other Blade Stations

In order to determine the slope of the lift curve, *a*, the Mach number effects were neglected (i.e. $M = 0$), in Equation 2-8. This resulted in a value of *a* equal to approximately 5.7 per radian or 0.1 per degree. Although this calculation was not necessary due to the given data Johnson (i.e. a = 5.7), it is included in the spreadsheet for future use if Mach number effects were to be considered.

$$C_l = \left[\frac{0.1}{\sqrt{1 - M^2}} - 0.01M \right] \alpha_{eff}$$

Equation 2-8: Coefficient of Lift

In order to continue, it was necessary to necessary to utilize the assumed values of C_T mentioned prior. Due to the fact that the blade is linearly twisted with a constant chord, Equation 2-9 was used to calculate the pitch of the blade at the 75% radius.

$$\theta_{0.75} = \frac{6C_T}{a\,s} + \frac{3}{2}\sqrt{\frac{C_T}{2}}$$

Equation 2-9: 75% Radius Linear Blade Pitch

Utilizing the twist angle, the blade pitch at each station was calculated with Equation 2-10.

$$\theta = \theta_{0.75} + (x_n - 0.75)\theta_{tw}$$

Equation 2-10: Blade Pitch

For each assumed value of C_T, an induced velocity was calculated as seen in Equation 2-11. Due to uniform inflow, this remained constant. As can be seen in Equation 2-11, the empirical k factor was utilized to account for non-uniform inflow and swirl losses. The value used in the Blade Element Theory cases was 1.07 (i.e. 1.1 - B^{-1}). Tip losses will be accounted for by altering the integration limits of C_T and C_{Pi}. This will be examined later in this section.

$$\lambda_i = \frac{v}{\Omega R} = k\sqrt{\frac{C_T}{2}}$$

Equation 2-11: Inflow

The induced angle of attack was than calculated with Equation 2-12.

$$\alpha_i = \tan^{-1}\left(\frac{v}{\Omega r}\right) = \tan^{-1}\left(\frac{v/\Omega R}{\Omega r/\Omega R}\right) = \tan^{-1}\left(\frac{\lambda_i}{x_n}\right)$$

Equation 2-12: Induced Angle of Attack

With θ and α_i now known, the effective angle of attack is as follows:

$$\alpha_{eff} = \theta - \alpha_i$$

Equation 2-13: Effective Angle of Attack

It was then necessary to calculate the coefficients of lift and drag with Equation 2-8 and Equation 2-14 respectively. The drag polar given in Equation 2-14 results in slightly different values than the one utilized in Johnson, but the difference is negligible.

$$C_d = 0.0081 + \left(65.8 a_{eff}^{\ 2} - 0.226 a_{eff}^{\ 4} + 0.0046 a_{eff}^{\ 6}\right)10^{-6}$$

Equation 2-14: Coefficient of Drag

The expressions for thrust and power were a bit more complicated. Equation 2-15 represents the differential thrust, with $f = 0$ for hover.

$$dT = \frac{1}{2} r V_{app}^{\ 2} c\left[C_l \cos(f + a_i) - C_d \sin(f + a_i)\right]dr$$

Equation 2-15: Differential Thrust

With $V_{app}^{\ 2} = \Omega^2 r^2$ and $x = \frac{r}{R} \Rightarrow dr = dxR$, Equation 2-15 was non-dimensionalized and resulted in the following:

$$dC_T = \frac{1}{2}\frac{c}{pR} x^2\left[C_l \cos(f + a_i) - C_d \sin(f + a_i)\right]dx$$

Equation 2-16: Differential Coefficient of Thrust

Integrating results in Equation 2-17.

$$C_T = b\sum \frac{1}{2}\frac{c}{pR} x^2\left[C_l \cos(f + a_i) - C_d \sin(f + a_i)\right]dx$$

Equation 2-17: Coefficient of Thrust

Simplifying, with solidity, $s = \frac{bc}{pR}$, results in the final expression for the coefficient of thrust.

$$C_T = \frac{s}{2}\sum x^2\left[C_l \cos(f + a_i) - C_d \sin(f + a_i)\right]dx$$

Equation 2-18: Coefficient of Thrust

In order to account for tip losses (B = 0.97), the expression for C_T was numerically integrated from the cutout to 0.97*R*. This was accomplished by merely "shrinking" the *dx* at the last blade station analyzed.

The power can be analyzed in a similar manner as seen below:

$$dP = (\Omega r)\frac{1}{2} r V_{app}^{\ 2} c\left[C_d \cos(f + a_i) + C_l \sin(f + a_i)\right]dr$$

$$dC_P = \frac{1}{2}\frac{c}{pR} x^3\left[C_d \cos(f + a_i) + C_l \sin(f + a_i)\right]dx$$

$$C_P = b\sum \frac{1}{2}\frac{c}{pR}x^3\left[C_d \cos(f + a_i) + C_l \sin(f + a_i)\right]dx$$

$$C_P = C_Q = \frac{s}{2}\sum x^3\left[C_d \cos(f + a_i) + C_l \sin(f + a_i)\right]dx$$

Equation 2-19: Coefficient of Power

In order to apply tip losses to the induced power only, it was necessary to divide the total power equation into its induced and profile components. As was done with thrust, the induced power, C_{Pi}, was then integrated to from the cutout to $0.97R$.

$$C_{Pi} = \frac{s}{2}\sum x^3\left[C_l \sin(f + a_i)\right]dx$$

Equation 2-20: Induced Power

$$C_{Po} = \frac{s}{2}\sum x^3\left[C_d \cos(f + a_i)\right]dx$$

Equation 2-21: Profile Power

Summing up the individual values of C_T and C_P at each of the blade stations resulted in a new value of total C_T and a value of total C_P for plotting purposes.

2.2.3. Combined Blade Element Theory

The major difference in Combined Blade Element (CBE) theory is the use of a non-uniform inflow calculation. The expression in Equation 2-22 below is derived as the result of equating the differential thrust from blade element and momentum theory.

$$l = \sqrt{\left(\frac{sa}{16} - \frac{l_c}{2}\right)^2 + \frac{sa}{8}qx} - \left(\frac{sa}{16} - \frac{l_c}{2}\right)$$

Equation 2-22: Non-Uniform Inflow Distribution

In addition, the value utilized for $q_{0.75}$ was not assumed utilizing Equation 2-9. This value was solved for utilizing the Excel Solver to obtain a converged solution where our $C_{Tnew} \cong C_{Tassumed}$. For general purpose, I also examined the results utilizing Equation 2-9 and the difference was negligible.

2.2.4. Summary Data

A summary of all data needed for plotting purposes is included in Table 2-1.

C_T/σ (assumed)	0.02	0.04	0.06	0.08	0.1
C_T (assumed)	0.002	0.004	0.006	0.008	0.010
#2 Simple Estimate, with k correction of:			**1.10**		
C_P	0.000195	0.000322	0.000486	0.000682	0.000903
C_P/σ	0.001946	0.003218	0.004865	0.006816	0.009028
C_T/σ	0.02	0.04	0.06	0.08	0.1
#2 Blade Element (with k correction of 1.07 and tip loss INT correction)					
TOTAL $C_{T\ (new)}$	0.001678	0.003356	0.005074	0.006810	0.008557
TOTAL $C_P = C_Q$	0.000159	0.000266	0.000409	0.000580	0.000778
C_P/σ	0.001588	0.002659	0.004085	0.005803	0.007781
C_T/σ	0.016780	0.033565	0.050741	0.068103	0.085567
#2 Combined Blade Element (non-uniform inflow and tip loss INT correction)					
TOTAL $C_{T\ (new)}$	0.002000	0.004000	0.006000	0.008000	0.010000
TOTAL $C_P = C_Q$	0.000169	0.000295	0.000463	0.000665	0.000897
C_P/σ	0.001689	0.002955	0.004634	0.006651	0.008973
C_T/σ	0.020000	0.040000	0.060000	0.080000	0.100000

Table 2-1: Compiled Hover Performance Data

2.2.5. Hovering Performance Plot

The required plot is represented in Figure 2-3 below.

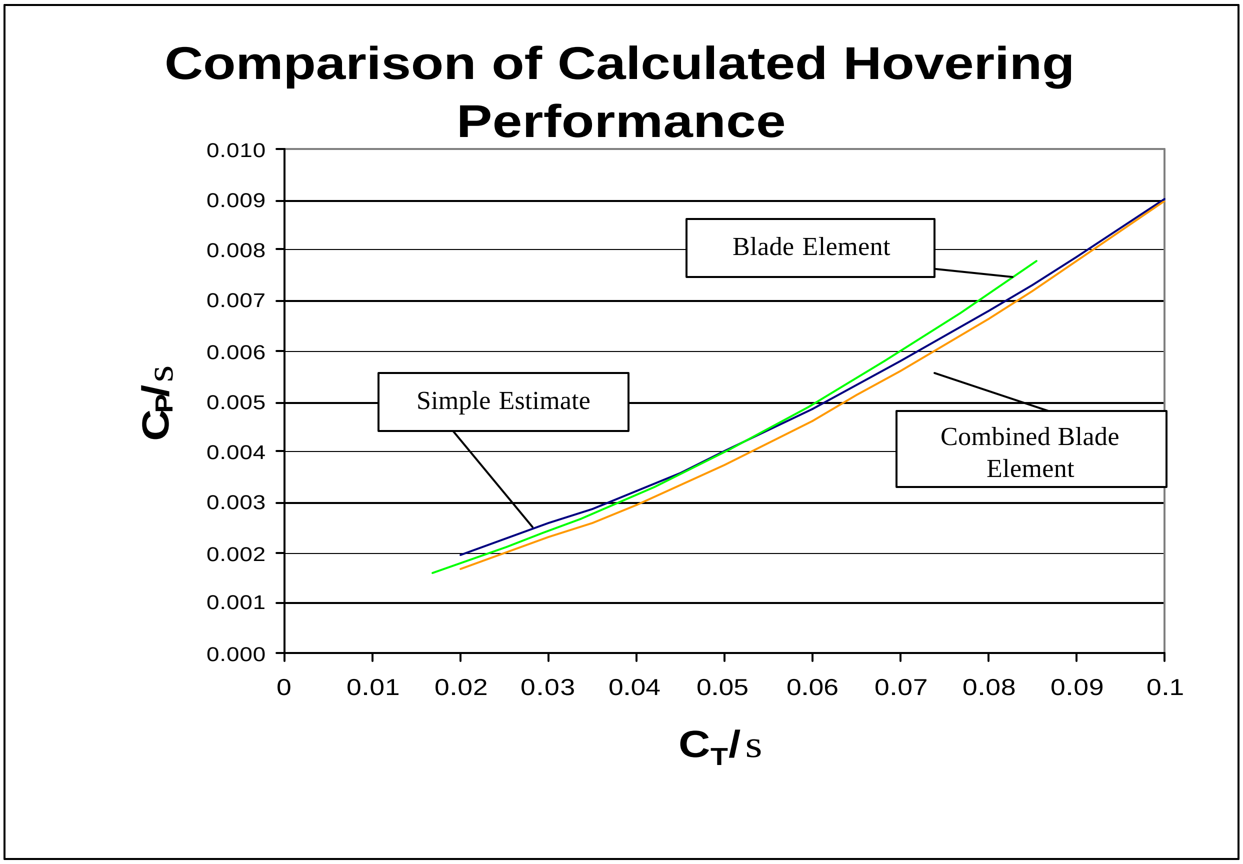

Figure 2-3: Comparison of Calculated Hovering Performance

This plot is very similar to the plot generated in Johnson (Figure 2-11). Minor differences are attributed to the utilization of the empirical k factor of 1.07 in Blade Element Theory. In addition, accounting for tip losses by altering the integration scheme at the tip, rather than merely applying an additional *k* factor would also cause slight differences. The result is a slight shift in the blade element curve appropriately (i.e. intersection with the simple estimate occurs at higher values of C_T/σ with decreasing k factor, as expected). Also, the drag polar utilized was not the same as Johnson (although very similar).

As discussed in Johnson (pg. 72), the differences between the simple estimate and the blade element curves are due to the profile power calculations. The difference between the blade element and the combined blade element curves are due to the non-uniform inflow of the combined blade element calculations.

2.3. Part 3)

2.3.1. Combined Blade Element Theory with a Tapered Blade

To execute the third part of this problem, it was necessary to develop a relationship for chord as a function of blade station, based on a 3:1 taper ratio. This result is then used to derive an expression for solidity relative to each blade station. The resulting expression is defined in Equation 2-23 below.

$$s_{new} = s_{old}\left[\frac{n_2 - n_1}{1 - cutout}x + \left(\frac{n_2 - n_1}{1 - cutout}cutout(-1) + n_1\right)\right]$$

Equation 2-23: Variable Chord (Tapered Blade)

The coefficients n_1 and n_2 are dependent upon the taper ratio and are calculated utilizing geometry (area of a trapezoid). When they are multiplied by the chord of the original blade, they result in the chord of the root and the tip of the tapered blade.

All other calculations utilized follow from Combined Blade Element theory (without taper), described prior.

In order to obtain a converged solution, the Excel Solver was once again used to determine a collective input angle that resulted in a C_T approximately equal to the C_T assumed. (0.07 in this case). The resulting angle was ≅ 11.02 degrees.

The calculated value for C_P was then compared with the CBE solution from the second part of this problem to compare the power reduction (or savings), due to the tapered blade.

#2 Combined Blade Element (non-uniform inflow and tip loss INT correction)					
TOTAL $C_{T\ (new)}$	0.002000	0.004000	0.006000	0.008000	0.010000
TOTAL $C_P = C_Q$	0.000169	0.000295	0.000463	0.000665	0.000897
C_P/σ	0.001689	0.002955	0.004634	0.006651	0.008973
C_T/σ	0.020000	0.040000	0.060000	0.080000	0.100000
#3 Combined Blade Element w/taper (non-uniform inflow and tip loss INT correction)					
C_P/σ	0.005289414				
C_T/σ	0.070000011	Only calculated for C_T/σ = 0.07			
Interpolation to find power reduction with taper:					
$C_P/\sigma_{\ interp}$	0.00564257	From #2 CBE			
Power Reduction	6.26%				

Table 2-2: Tapered Blade Analysis

As can be seen from Table 2-2, the tapered blade resulted in a reduction in power of ≅ 6.26%. This is slightly higher than the value presented in Johnson of 5.5%. The slight difference could be attributed to the factors discussed prior in the blade element section, as well as due to round-off error in my computer calculations.

Overall, it has been shown that twist and taper can be combined to improve the performance of the rotor. The trade-offs are both performance and cost related. Twisting increases the vibration in forward flight and also has a negative impact on the autorotational index. Taper is primarily an affordability issue due to the high cost of manufacturing tapered blades versus the gain in performance seen on the aircraft (i.e. higher forward flight airspeeds).